Table III. Calculated and Experimental Spin Densities and Proton Splittings for the BaP Cation Radical

position	calcd spin density (ρ)	calcd proton splitting[a]	exptl spin density	exptl proton splitting
1	0.1555	4.35	0.163	4.57
2	-0.0403	1.13	(-)0.0193	0.54
3	0.1396	3.92	0.135	3.77
4	0.0890	2.49	0.0133	0.37
5	0.0858	2.40	0.0743	2.11
6	0.2633	7.37	0.237	6.63
7	0.0872	2.44	0.0793	2.23
8	-0.0172	0.48	(-)0.0067	0.19
9	0.0583	1.63	0.105	2.95
10	0.0144	0.40	0.0693	1.94
11	0.0143	0.40	(-)0.0294	0.824
12	0.1084	3.03	0.0971	2.75

[a] Calculated from McConnell's equation $|a| = Q|\rho|$, Q = 28 G.

overestimating at the 4 position. Attempts to improve the calculations by allowing the overlap integrals to vary according to the known bond lengths[22] of the BaP molecule did not result in any better agreement. Other more sophisticated calculations of electron densities in the HOMO of BaP, also carried out on idealized geometries, are also in no better agreement with the experimental values.[5,23] Since the spin densities represent one-half of the electron density in the HOMO, and since the latter have been related to the nucleophilic reactivity at the carbon atoms,[5,6] the observed deviations between the calculated and experimental values could have a significant effect on interpretations or rationalizations of metabolic pathways based on calculated values. For example, the high spin density observed at the 9 position could indicate that direct oxygen insertion to form 9-hydroxybenzo[*a*]pyrene may account for part or all of the observed metabolic production of this phenol. Additionally the experimentally observed inequivalence of the 4 and 5 positions which was suggested by our previous studies[11,12] of methylated BaP's is supported by the ^{13}C studies. This inequivalence, which is not reproduced by any method of calculation so far investigated would explain the selective production of 5-hydroxybenzo[*a*]pyrene from the isomerization of benzo[*a*]pyrene 4,5-oxide or from the acid dehydration of benzo[*a*]pyrene-4,5-diol.[24] It is also consistent with the breaking of the C_4-O bond in the enzymatic hydrolysis of benzo[*a*]pyrene 4,5-oxide as observed by Yang et al.[24] However, similar selectivity was not observed by Hylarides et al.[25] in their study of BaP-4,5-oxide.

It is obvious from these results that great care should be exercised when using calculated parameters to explain the biological properties of complex molecules. Experimentally derived quantities such as the HOMO spin densities are important in providing a test for the validity of such calculations, and the values obtained in this work should provide a useful set of data against which more refined calculations can be compared.

Acknowledgment. This work was supported, in part, by Grant CA-34966 awarded by the National Cancer Institute, DHEW, to P.D.S.

Registry No. 1-^{13}C-BaP, 93604-46-7; 2-^{13}C-BaP, 93604-47-8; 3-^{13}C-BaP, 93604-48-9; 4-^{13}C-BaP, 67194-47-2; 5-^{13}C-BaP, 67194-48-3; 6-^{13}C-BaP, 77585-09-2; 7-^{13}C-BaP, 87337-12-0; 8-^{13}C-BaP, 87337-13-1; 9-^{13}C-BaP, 87337-14-2; 10-^{13}C-BaP, 87337-15-3; 11-^{13}C-BaP, 67194-49-4; 12-^{13}C-BaP, 67194-50-7; ^{13}C, 14762-74-4.

(22) Iball, J.; Scrimgeour, S. N.; Young, D. W. *Acta Crystallogr., Sect. B* **1976**, *32*, 328-330.
(23) Shipman, L. L.; In "Carcinogenesis. A comprehensive Survey"; Jones, P. W., Freudenthal, R. I., Eds.; Raven Press: New York, 1978; Vol., 3, pp 139-144.
(24) Yang, S. K.; Roller, P. P.; Gelboin, H. V. *Biochemistry* **1977**, *16*, 3680-3687.
(25) Hylarides, M. D.; Lyle, T. A.; Daub, G. H.; VanderJagt, D. L. *J. Org. Chem.* **1979**, *44*, 4652-4657.

An Advanced Visible-Light-Induced Water Reduction with Dye-Sensitized Semiconductor Powder Catalyst

Takeo Shimidzu,* Tomokazu Iyoda, and Yoshihiro Koide

Contribution from the Division of Molecular Engineering, Graduate School of Engineering, Kyoto University, Sakyo-ku, Kyoto 606, Japan. *Received June 20, 1984*

Abstract: For visible-light-induced water reduction to hydrogen with use of a sacrificial electron donor (triethanolamine), an efficient and durable photocatalyst system with xanthene dye sensitization of particulate platinized semiconductor catalyst is presented. A reductive electron-transfer mechanism from the photoreduced dye to the particulate platinized semiconductor is proposed in the present hydrogen production. The excited triplet state of the dye is a precursor of the reduced dye by the amine, so that the efficiency is determined mainly by the real excited triplet quantum yield of the dye. On the basis of this consideration, a novel use of heavy-atom additives to increase the efficiency of durable xanthene dye sensitized systems is demonstrated.

Significant progress on the photoinduced water reduction to hydrogen has been made independently by two main approaches using a sacrificial electron donor. One is the heterogeneous system, in which a particulate (platinized) semiconductor catalyst (Sc or Sc/Pt) is suspended, with band-gap excitation,[1] and the other is a homogeneous photoinduced redox system containing a sensitizer, an electron relay, and a microdispersed Pt catalyst.[2] However, they have some defects: The former has photoaction with near-UV light and tends to photocorrode with photogenerated positive holes in Sc, and the latter has no anisotropic reaction fields available for charge separation.

(1) Since the Honda-Fujishima effect (Honda, K.; Fujishima, A. *Nature (London)* **1972**, *238*, 37), numerous investigations have been done. So, some reviews are listed herein. (a) Heller, A. *Acc. Chem. Res.* **1981**, *14*, 154. (b) Wrighton, M. S. *Acc. Chem. Res.* **1979**, *12*, 303. (c) Bard, A. J. *J. Photochem.* **1979**, *10*, 59. (d) Memming, R. *Electroanal. Chem.* **1979**, *11*, 1.

(2) Grätzel, M.; Kalyanasundaram, K.; Kiwi, J. "Structure and Bonding. 49. Visible Light Induced Cleavage of Water into Hydrogen and Oxygen in Colloidal and Microheterogeneous System"; Springer-Verlag: New York, 1982.

0002-7863/85/1507-0035$01.50/0

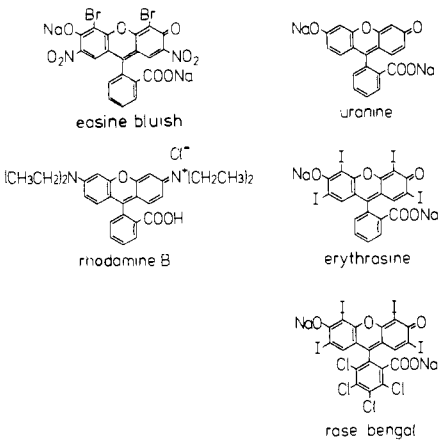

Figure 1. The structures of some xanthene dyes adopted as a sensitizer in the present hydrogen production.

A third approach, the dye sensitization of a particulate Sc or Sc/Pt catalyst, has been proposed in an attempt to combine these two methods. This catalyst system has the ability of using a visible-light-responsive sensitizer and an anisotropic reaction field, i.e., Schottky-type potential barrier, at the semiconductor/liquid interface. Up to date, few visible-light-induced hydrogen production systems based on the third approach have been demonstrated,[3,4] although its concept has been established already in the field of *bulky* semiconductor electrodes[5] and photographic chemistry.[6]

As reported previously,[3] visible-light illumination ($500 < \lambda < 700$ nm) of a water-soluble porphyrin zinc complex and triethanolamine (TEA) in aqueous solution (pH 8) suspending particulate Sc/Pt resulted in efficient hydrogen production ($\Phi_{H_2} > 0.03$ at 548 ± 3 nm with $ZnTPPS_4$–ZnO/Pt catalyst). Compared with lower apparent current quantum efficiency[7] in dye sensitization of *bulky* semiconductor electrodes where the photocurrent is generated through oxidative electron transfer, the success in high hydrogen production yield should be explained by an alternative mechanism. This is the reductive electron transfer mechanism where an excited sensitizer is reduced with electron donor and the reduced sensitizer acts as an electron-injecting species. This approach can be applied to other sensitizers and other Sc supports, so the authors have dealt with some xanthene dyes as sensitizers in order to explore the mechanism and the requirements for working the catalyst.[4c] Among them, rose bengal or erythrosine–ZnO/Pt catalyst produced hydrogen in remarkably high quantum yield ($\Phi_{H_2} > 0.26$ at 520 ± 3 nm). However, the catalysis reactions with both xanthene dyes were accompanied with their photodehalogenation, and this defect should be overcome.

Here, we report extensive studies on the visible-light-induced water reduction with some xanthene dye-sensitized particulate Sc/Pt catalysts, especially on comparisons of their efficiencies. The reductive electron-transfer mechanism through the excited triplet state, in which the one-electron reduced dye with the amine is an electron-injecting species to particulate Sc/Pt, is proposed. Also, the present paper describes a novel use of heavy-atom additives to increase the efficiency of durable xanthene dye sensitized systems for the photoreduction of water.

Scheme I. The Apparatus in the Transient Absorption Measurement[a]

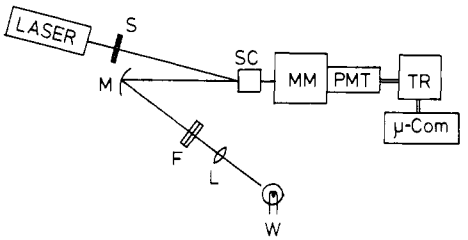

[a] S, shutter; M, mirror; SC, sample cell; F, filters (Toshiba, UVD33s and UV35, optical window, $350 < \lambda < 400$ nm); L, lens; MM, monochromator fixed at 393 nm (Nikon G-250); PMT, photomultiplier tube (Hamamatsu Photonics, 1P28); μ-Com, microcomputer (Sharp MZ-80c); W, 40-W tungsten lamp; LASER, argon ion laser (Spectra Physics, 165, 488 nm, 0.2 W).

Experimental Section

Materials. Among xanthene dyes, uranine, rhodamine B, eosine bluish (Nakarai Chemical), erythrosine (Merck), and rose bengal (Schmid GMBH&Co.) were adopted in the present study (Figure 1). Various semiconductor powders (Sc, ca. 100 mesh) were of commercial origin (Nakarai Chemical, >99.5% of purity). The platinized semiconductor (Sc/Pt) was prepared in a manner similar to that described earlier.[3] The amount of Pt adhered to Sc was expressed by means of the weight ratio of Pt to Sc in grinding. The catalytic activity of Sc/Pt was reproduced within ±5%, judging from the hydrogen production. Triethanolamine (TEA) and the other chemicals were of the best commercial grades (Nakarai Chem. and Wako Chem.)

Photolysis Procedure. A standard photolysis solution (5 mL) contained a sensitizer (4.0×10^{-4} mol·L^{-1}), TEA (2.0×10^{-1} mol·L^{-1}), and Sc/Pt (5 or 10 wt % Pt, 6 mg·mL^{-1}) in a Pyrex test tube (head space, 28.5 mL). The deaerated solution after 20 min of bubbling with Ar was photolyzed with UV and IR cutoff filters (Toshiba, L42 and IR25s: $420 < \lambda < 700$ nm of optical window) with magnetic stirring to suspend Sc/Pt. In measuring the apparent quantum yield (Φ_{H_2}), the deaerated photolysis solution (5 mL), in a square quartz cell, was illuminated with monochromatic light (±3 nm of bandwidth; 3 mm × 20 mm of incident light area) through a CT-25N grating spectroscope (Japan Spectroscopic). The apparent quantum yield (Φ_{H_2}, μmol($^1/_2H_2$)·einstein^{-1} of unit) was introduced, which is defined as the following equation (eq 1).

$$\Phi_{H_2} = \frac{2(\text{mol of hydrogen})}{(\text{mol of incident photon})} \quad (1)$$

Since the photolysis solution was heterogeneous, we estimated it by assuming that all the incident photons were completely absorbed by a sensitizer and no correction was made for light reflected and scattered by particulate Sc/Pt. The photon flux of the incident light was determined by Reinecke's chemical actinometry.[8]

Measurements. Hydrogen was analyzed with a GC-3BT gas chromatograph (Shimadzu) equipped with 2 m of molecular sieves 5A (Nishio) at 100 °C. The initial hydrogen production rates (r_0) were adopted in order to compare catalytic activities and to eliminate any factors of decreasing the rate such as the consumption of a sacrificial electron donor, the deterioration of a dye, etc. Except heavy-halogenated xanthene dyes, the obtained r_0's were valid for 15 h of photolysis. The photolyzed solution was analyzed with an LC-3A HPLC instrument (Shimadzu) with use of a Nucleosil $7C_{18}$ column (Macherey-Nagel). The solvent was 70% methanolic aqueous solution containing 5.0×10^{-4} mol·L^{-1} tetrabutylammonium phosphate (Waters) as a paired ion reagent. The isotope distribution of the hydrogen from H_2O–D_2O (1:1) was determined with an M-80A mass spectrometer (Hitachi), assuming that H_2, HD, and D_2 have the same sensitivity. The calibration of hydrogen was carried out by using standard hydrogen gas (H_2, 99.9999% of purity), and the correction of the diffusion constant ($\propto$ (molecular weight)$^{1/2}$) of each gas was made.

Cyclic voltammograms of the adopted xanthene dyes were recorded on a NPGS-301 potentiogalvanostat and a NFG-3 function generator (Nikkokeisoku) with use of SCE as a reference electrode.

Visible absorption spectra were recorded on a SM-401 spectrophotometer (Union Giken). Luminescence spectra were recorded with a 150 W Xe lamp, an M-200 microcomputer (SORD), and a near-IR photon-counting instrument (Unisoku, Type I) which consisted of an R-316 photomultiplier tube (Hamamatsu Photonics) and a 520-29-110 dif-

(3) Shimidzu, T.; Iyoda, T.; Koide, Y.; Kanda, N. *Nouv. J. Chim.* **1983**, *7*, 21.
(4) (a) Hashimoto, K.; Kawai, T.; Sakata, T. *Nouv. J. Chim.* **1983**, *7*, 249. (b) Grätzel, M.; Kalyanasundaram, K. *Angew. Chem., Int. Ed. Engl.* **1979**, *18*, 701. (c) Shimidzu, T.; Iyoda, T.; Koide, Y.; Kanda, N. 46th Annual Meeting of the Chemical Society, Japan, (Niigata), Preprints, p 118 (1982, September).
(5) Tsubomura, H. "Photoelectrochemistry and Light Energy Conversion"; Tokyo Kagaku Dojin: Tokyo, 1980.
(6) Mees, C. E. K.; James, T. H. "The Theory of the Photographic Process", 3rd ed.; Macmillan: New York, 1966.
(7) Matsumura, M.; Nomura, Y.; Tsubomura, H. *Bull. Chem. Soc. Jpn.* **1977**, *50*, 2533.
(8) Wegner, E. E.; Adamson, A. W. *J. Am. Chem. Soc.* **1966**, *88*, 394.

Table I. The Results of Visible-Light-Induced Hydrogen Production Catalyzed by Xanthene Dyes–Platinized Semiconductor–TEA under Visible-Light Illumination[a]

xanthene dye	rates of H_2 production (μmol·min^{-1}) for the following platinized semiconductors				
	ZnO/Pt	TiO_2/Pt	SnO_2/Pt	CdS/Pt	Fe_2O_3/Pt
rose bengal	1.23	0.24	0.37	0.28	0.54
eosine bluish	0.16	0.04	0.05	0.03	0.07
uranine	0.09	0.08	0.06	0.03	0.02
rhodamine B	0.01	<0.01	0.00	0.01	<0.01
none	0.00	0.00	0.00	0.01	0.00
none[b]	trace	0.02	0.00	0.01	0.00

[a] The initial rates were estimated from the detailed time courses of hydrogen production. 5 mL of the photolysis solution contained 4.0×10^{-4} mol·L^{-1} of xanthene dye, 2.0×10^{-1} mol·L^{-1} of TEA, and 30 mg of platinized (10 wt %) semiconductor powder in deaerated neutral aqueous solution. Steady illumination was employed with a 500-W Xe lamp through a 420-nm cutoff filter. [b] Through a 300-nm cutoff filter, i.e., in the case of band-gap excitation without sensitization.

fraction grating (Jobin Yvon). The deaerated aqueous solution of the dye was placed in a square quartz cell (optical path, 1 cm) in measuring the emission spectrum at room temperature. The emission spectrum at 77 K was measured in a 2-mm-radius round quartz cell kept in liquid N_2. The sample was degassed by 3 cycles of the freeze–pump–thaw method. The mixture of triply distilled water and distilled ethyleneglycol (50 v/v %) was used as a glassy solvent. The experimental setup in the transient absorption measurement is shown in Scheme I. The light source was an argon ion laser (Spectra Physics, 165; 488 nm, 0.2 W). The photolysis solution contained 4.0×10^{-4} mol·L^{-1} of uranine, 2.0×10^{-1} mol·L^{-1} of TEA, and 2.0×10^{-1} mol·L^{-1} of I^-, whose concentrations were adjusted to those in hydrogen production. The analyzing optical system consisted of a 40 W tungsten lamp equipped with filters (Toshiba, UVD33s and UV35; $350 < \lambda < 400$ nm of optical window), a monochromator (Nikon G-250), and a 1P28 photomultiplier tube (Hamamatsu Photonics). Time dependence of the absorbance was recorded on an M-50E transient recorder (Kawasaki Electronica) and analyzed with an MZ-80c microcomputer (Sharp). The photolysis solution was deaerated with N_2 bubbling for 15 min or degassed by the freeze–pump–thaw method.

Results and Discussion

(1) Visible-Light-Induced Hydrogen Production with Xanthene Dye–Sc/Pt Catalyst. Visible-light illumination ($420 < \lambda < 700$ nm) of xanthene dye (4.0×10^{-4} mol·L^{-1}) and TEA (2.0×10^{-1} mol·L^{-1}) in aqueous solution (5 mL, pH 8) suspending particulate Sc/Pt (5 or 10 wt % Pt, 6 mg·mL^{-1}) resulted in efficient hydrogen production. Table I shows a list of the initial hydrogen production rates (r_0) with various xanthene dye–Sc/Pt catalysts with TEA as a sacrificial electron donor. As with the $ZnTPPS_4$–Sc/Pt catalysts in our preceding report,[3] the blank experiments showed the following observations: (i) No hydrogen was produced when xanthene dye, Sc/Pt, TEA, or visible-light illumination was lacking. (ii) Sc suspension without adhering Pt or Pt black suspension without Sc supports had little catalytic activity (<0.01 μmol·min^{-1}). The simple mixture of Sc and Pt black without grinding them together worked badly as the catalyst (<0.01 μmol·min^{-1}). On the contrary, the adhesion (5–10 wt %) of slight Pt to Sc supports[9] enhanced the catalytic activity up to 100–150 times. (iii) The action spectra of the hydrogen production agreed with the visible absorption spectra of the adopted dyes (for example, Figure 3 (- - -●- - -) in rose bengal–ZnO/Pt catalyst). (iv) Band-gap exctation (>300 nm) of TEA aqueous solution suspending ZnO/Pt, TiO_2/Pt, and CdS/Pt without dye sensitization resulted in a smaller amount of hydrogen production (Table I, the lowest line) than that by the present dye-sensitized system. (v) The mass spectrometric analysis of the hydrogen produced in H_2O–D_2O (1:1 v/v) solution resulted in the isotope distribution: H_2:HD:D_2 = 23:62:15 (apparent vol %). These observations illustrate that xanthene dye sensitized electron transfer to particulate Sc/Pt results in water reduction to produce hydrogen and that Sc/Pt plays a significant role as a proton-reducing catalyst and/or an electron relay.

Two main observations are drawn in Table I. Firstly, the xanthene dye bearing more heavy-halogen substitutents in its basic structure had larger r_0's. Secondly, large differences in catalytic

(9) When Sc/Pt was prepared by a photoplatinization method (Kraeutler, B.; Bard, A. J. *J. Am. Chem. Soc.* **1978**, *100*, 4317), about 0.1% adhesion of Pt on Sc made the Sc/Pt act as an effective proton-reducing catalyst.

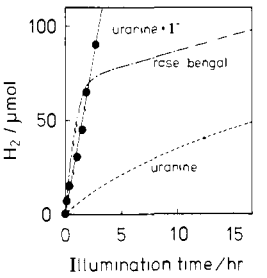

Figure 2. The time courses of the hydrogen production with rose bengal– (- - -) or uranine– (- - -) ZnO/Pt–TEA systems and with uranine–ZnO/Pt–TEA–I^- (●). [dye] = 4.0×10^{-4} mol·L^{-1}, [TEA] = 0.2 mol·L^{-1}, ZnO/Pt (10 wt % Pt) 6 mg·mL^{-1}. The deaerated photolysis solution (5 mL) was illuminated with >420 nm.

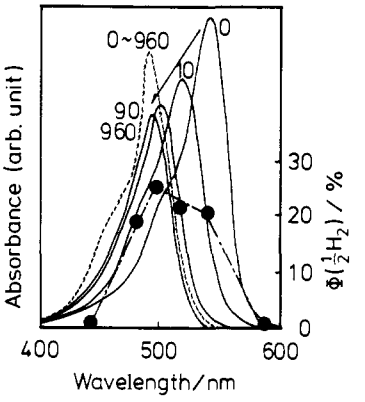

Figure 3. The visible absorption spectra of the photolysis solution in rose bengal– (—) or uranine– (- - -) ZnO/Pt–TEA systems and the action spectrum of hydrogen production with rose bengal–ZnO/Pt–TEA (- - -●- - -) The figures show the illumination time (min) under the present conditions.

activities are observed among the various Sc supports. Unfortunately, the energetics of the reltive positions of the band-edge energy of Sc and the redox potentials of the electron-injecting species fails to explain both observations, as will be described later in a section 3.

Here, the detailed experiments on the former are developed, focussing on the action of heavy-halogen substituents in the adopted xanthene dyes. Figure 2 shows the time courses of the hydrogen production sensitized with rose bengal (heavy-halogenated xanthene dye, - - -) and uranine (nonhalogenated xanthene dye, - - -) with use of the excellent ZnO/Pt catalyst. While uranine–ZnO/Pt catalyst produced hydrogen at 0.09 μmol·min^{-1} almost steadily for over 16 h of illumination without any spectral changes, rose bengal–ZnO/Pt catalyst bearing large r_0 (1.23 μmol·min^{-1}) had a break point at 1.5 h under the present illumination conditions. The decreased rate (0.08 μmol·min^{-1}),, similar to r_0 with uranine–ZnO/Pt catalyst, was sustained for over 10 h after the break point. During the decrease of the rate, the maximum absorption of the photolysis solution gradually shifted from 548 to 492 nm (Figure 3, —). The final spectrum at the

break point agreed with that of uranine and afterwards little spectral change was observed. The action spectrum of hydrogen production with the rose bengal–ZnO/Pt catalyst located broadly from 550-nm region to the 470-nm region because of the deterioration of rose bengal and the apparent quantum yield (Φ_{H_2}) exceeded over 0.2 (Figure 3, - - -●- - -). In the uranine–ZnO/Pt catalyst system, the visible absorption spectrum during the photolysis indicated no photodeterioration of the uranine. The HPLC analysis of the photolyzed solution with the rose bengal–ZnO/Pt catalyst showed, judging from the retention time,[10] that rose bengal is converted to a dehalogenated uranine-like structure. About 6 equiv of halide ions to rose bengal was detected in the bleached solution by means of gravimetry with silver nitrate at the break point in the time course (Figure 2, - - -). Rose bengal is photodehalogenated in the first stage, competing with the desired hydrogen production. Since r_0 of the rose bengal–ZnO/Pt catalyst was proportional to the concentration of rose bengal up to 4.0×10^{-4} mol·L^{-1}, the decrease of the rate during the photolysis resulted from the conversion of rose bengal into a uranine-like structure bearing moderate catalytic activity. These phenomena were also observed in other heavy-halogenated xanthene dye-sensitized catalysts, independent of the variety of Sc/Pt. Nonhalogenated xanthene dye-sensitized catalysts were durable against any deterioration, maintaining their moderate catalytic activities. Heavy-halogen substituents in xanthene dyes play a significant role in enhancing the intrinsic catalytic activity, which results from the internal heavy-atom effect.[11] As for the photodeterioration of heavy-halogenated xanthene dyes,[19] a one-electron reduced xanthene dye with alcohol is dehalogenated with another excitation. The photoreduction of the dye occurred through its excited triplet state (T_1).

(2) External Heavy-Atom Effect on the Present Hydrogen Production. Heavy-halogenated xanthene dyes have larger r_0's with the internal heavy-atom effect but unfortunately tend to photoeliminate their heavy-halogen substituents in the presence of a reducing agent, followed by a decrease of their r_0's. Alternatively, we applied the external heavy-atom effect[11d] in order to increase the efficiency of the non-halogenated xanthene dye-sensitized catalysts which are durable against photodeterioration. The addition of I^- (2.0×10^{-1} mol·L^{-1}) in uranine–ZnO/Pt catalyst enhanced the hydrogen production rate by over 11 times, up to 1.04 μmol·min^{-1} ($\Phi_{H_2} > 0.22$ at 492 ±3 nm) (Figure 2, -●-). During the photolysis, no decrease of the enhanced r_0 and no photodeterioration were observed. The visible absorption spectrum of the photolysis solution was independent of the addition of I^- and so was the action spectrum of the hydrogen production. No hydrogen was produced in uranine–ZnO/Pt–I^- without TEA. After 20 h the enhanced rate gradually decreased, but it was restored by the new addition of TEA, not by that of I^-. These observations suggested that the enhanced catalytic activity of uranine is explained by the external heavy-atom effect of the added I^-. In the case of rose bengal–ZnO/Pt catalyst, the enhancement was scarcely observed (1.20 μmol·min^{-1}), but the photodehalogenation was depressed slightly.

The addition of other halide ions also enhanced the hydrogen production rate, and this effect is represented by $F(X)$,

$$F(X) = r(X)/r_0 \qquad (2)$$

where r_0 and $r(X)$ are the hydrogen production rates in the absence and presence of an additive (X), respectively. $F(X)$ became greater for some halide ions; $1 < F(Cl^-) < F(Br^-) \ll F(I^-)$ (Figure 4). All $F(X)$'s increased linearly with the concentration of X, [X]. In $[I^-] < 2.0$ mol·L^{-1}, $F(I^-)$ had the maximum at 0.2 mol·L^{-1} (500 equiv of uranine), while no saturation was observed in $F(Cl^-)$ and

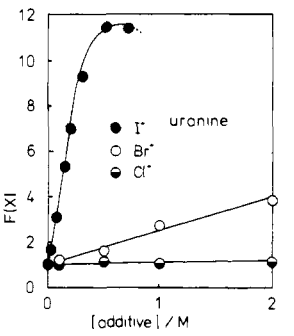

Figure 4. The dependence of the concentration of the added halide ions on the increase of the hydrogen production rates, $F(X)$'s. [uranine] = 4.0×10^{-4} mol·L^{-1}, [TEA] = 0.2 mol·L^{-1}, ZnO/Pt (10 wt % Pt) 5 mg·mL^{-1}. (●) I^-, (○) Br^-, (◒) Cl^-.

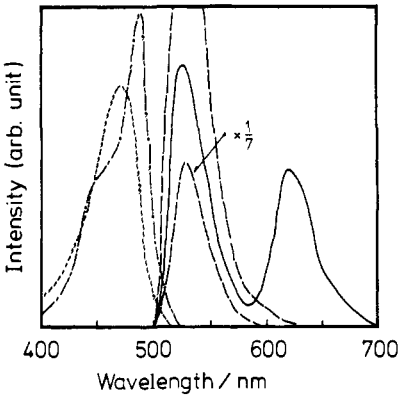

Figure 5. The emission spectra of uranine at 77 K in the absence (- -) and the presence (—) of I^-, exciting at 492 nm. (- - -) The excitation spectrum at 77 K in monitoring 620-nm emission. (- - -) The visible absorption spectrum of uranine.

$F(Br^-)$. Cs^+ and Xe also increased the rate.[12] The concentration of I^- and Cl^- released during the photodehalogenation was at most $\sim 10^{-3}$ mol·L^{-1}, so that the enhancement of the rate was not expected in the second stage (>1.5 h of photolysis) of the time course (Figure 2). As is familiar in organic photochemistry, the magnitude of the external heavy-atom effect, in unit amount of X, is much less than that of the internal effect.

When exciting at 492 nm, the fluorescence at 520 nm of uranine was efficiently quenched by I^- and Br^- but scarcely by Cs^+ and Cl^- within the limit of experimental error. Stern–Volmer analysis showed that the second-order quenching rate constants (k_q) were 9.2×10^9 for I^-, 7.1×10^7 for Br^-, and $<8.9 \times 10^6$ l·mol^{-1}·s^{-1} for Cs^+ and Cl^-, respectively, using 3.6 ns for the natural lifetime of the excited singlet uranine.[13] At 77 K a new emission at 620 nm, together with the 520-nm fluorescence, was observed in the presence of I^- and assigned to the phosphorescence of uranine or an exciplex localized on the excited triplet uranine[14] (Figure 5, —). The excitation spectrum obtained by monitoring the 620-nm emission agreed with the visible absorption spectrum of uranine (Figure 5, - - -). These observations coincided with an increase of real excited triplet quantum yield (Φ_{TM}) of uranine by the external heavy-atom effect of I^-. The heavy-atom effect involves the increase of the electronic transition probability between different spin multiplicities, not only $S_1 \rightarrow T_1$ but also $T_1 \rightarrow S_0$ and $S_0 \rightarrow T_1$.[11] Generally, it is reported that the $S_1 \rightarrow T_1$ process is more sensitive to the heavy-atom effect than the $T_1 \rightarrow S_0$ and the $S_0 \rightarrow T_1$ processes.[15] The transient absorption experiments on

(10) Rose bengal and uranine have 3.4 and 2.4 min of retention time, respectively, under 1.0 mL·min^{-1} of flow rate. The HPLC pattern of the photolysis solution after 10 min of illumination showed a new peak at 2.4 min of retention time.

(11) (a) Birks, J. B. "Photophysics of Aromatic Molecules"; John Wiley & Sons: New York, (1979). (b) McClure, D. S. *J. Phys. Chem.* **1949**, *17*, 905. (c) Ermolaev, V. L.; svitashev, K. K. *Opt. Spectrosc.* **1959**, *7*, 399. (d) Kasha, M. *J. Phys. Chem.* **1952**, *20*, 71.

(12) $F(Xe)$ and 1.01–1.05. The external heavy-atom effect of Xe was examined by replacing the atmosphere of the photolysis cell with Xe gas (Teikoku Sanso K.K.). The solubility of Xe gas in water is 4.95×10^{-3} mol·L^{-1} at 1 atm.

(13) Lessing, H. E. *J. Mol. Struct.* **1982**, *84*, 281.

(14) Koizumi, M. "Introduction of Photochemistry"; Asakura Japan, 1963; p 305.

(15) McGlynn, S. P.; Reynolds, M. J.; Daigre, G. W.; Christodoyleas, N. D. *J. Phys. Chem.* **1962**, *66*, 2499.

Table II. The Effect of the Addition of I^- on the Hydrogen Production Rates with Xanthene Dye–ZnO/Pt–TEA Systems[a]

xanthene dye	r_0, μmol·min^{-1}	$r(I^-)_{max}$, μmol·min^{-1}	$[I^-]$, mol·L^{-1}	$F(I^-)_{max}$	$\Phi°_{TM}$
uranine	0.09	1.04	2.0×10^{-1}	11.5	0.05
rhodamine B	0.01_1	1.28	2.0×10^{-1}	117.0	0.02
rose bengal	1.23	1.35	1.6×10^{-4}	1.1	0.98
erythrosine	1.34	1.34	4.0×10^{-2}	1.0	1.00

[a] The hydrogen production rates were estimated from the detailed time courses of hydrogen production. $r(I^-)_{max}$ and $[I^-]$ are the maximal hydrogen production rates enhanced by the addition of I^- and the concentration of I^- in observing $r(I^-)_{max}$. $\Phi°_{TM}$ shows the excited triplet quantum yield of the xanthene dye. 5 mL of the photolysis solution containing 4.0×10^{-4} mol·L^{-1} of a xanthene dye, 2.0×10^{-1} mol·L^{-1} of TEA, and 30 mg of platinized semiconductor powder catalyst in deaerated neutral aqueous solution. Steady illumination was employed with a 500-W Xe lamp through a 420-nm cutoff filter.

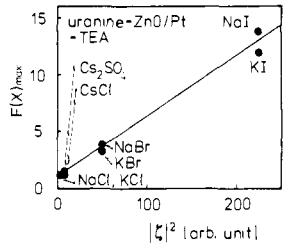

Figure 6. The relationship between $F(X)_{max}$ and $\{\zeta(X)\}^2$ in the hydrogen production by uraine–ZnO/Pt–TEA. $F(X)_{max}$ and $\{\zeta(X)\}^2$ show the maximum value of the observed $F(X)$ and the square value of the spin–orbit coupling constant of X, which were referred from ref 18.

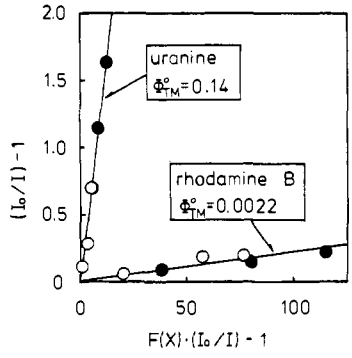

Figure 7. The Wilkinson-type plots in uranine and rhodamine B–ZnO/Pt–TEA systems.

the excited triplet uranine showed that I^- quenches the T_1 state of uranine to the S_0 but that its rate is smaller than the T_1 quenching with TEA,[16] followed by the generation of the uranine anion radical. When a strong heavy-atom such as I^- is added to the photolysis solution, the saturation or the decrease of $F(I^-)$ in higher concentration (>0.2 mol·L^{-1}) of I^- is due to the probability of T_1 quenching increasing with I^- (Figure 4).

The maximum of the observed $F(X)$, $F(X)_{max}$,[17] was proportional to the square of the spin–orbit coupling constant[18] of the adopted X, $\{\zeta(X)\}^2$. The value $\{\zeta(X)\}^2$ measures the magnitude of the heavy-atom effect with X (Figure 6).

The external heavy-atom effect was applied to explain the other xanthene dye sensitized catalysts. Uranine and rhodamine B have small $\Phi°_{TM}$ but large $F(I^-)_{max}$, while rose bengal and erythrosine have large $\Phi°_{TM}$ with $F(I^-)_{max}$ almost unity (Table II). The apparent quantum yields of the hydrogen production with both the formers, uranine–ZnO/Pt–I^- and rhodamine B-ZnO/Pt-I^-, exceeded 0.2, which are comparable with that of rose bengal–ZnO/Pt catalyst in its first stage. The hydrogen production rate and its enhancement by the external heavy-atom effect were very

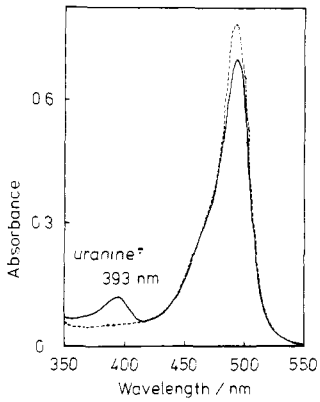

Figure 8. The visible absorption spectrum of the photolyzed uranine–TEA aqueous solution without Sc/Pt. [uranine] = 1.67×10^{-5} mol·L^{-1}, [TEA] = 0.33 mol·L^{-1}, pH 8.

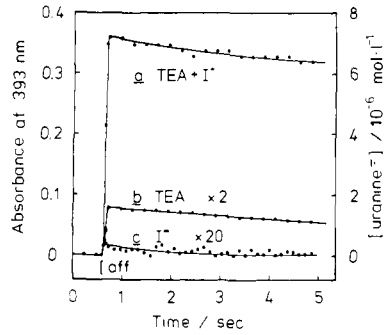

Figure 9. The time dependneces of the 393-nm absorbances assigned to uranine anion radical after 55 ms of illumination at 488 nm. (a) Uranine–TEA–I^-, (b) uranine–TEA, (c) uranine–I^-. [Uranine] = 4.0×10^{-4} mol·L^{-1}, [TEA] = 0.2 mol·L^{-1}, $[I^-]$ = 0.2 mol·L^{-1}.

sensitive to $\Phi°_{TM}$. Therefore, the mechanism of hydrogen production through the excited triplet state of the dye (T_1) as a key intermediate is proposed.

A Wilkinson-type analysis (eq 3) using the fluorescence quenching and the $F(X)$ for uranine and rhodamine B with ZnO/Pt was carried out in order to confirm the T_1-intermediate mechanism,[19] where I_0 and I are the fluorescence intensities in

$$(I_0/I) - 1 = [F(X)(I_0/I) - 1]\Phi°_{TM} \quad (3)$$

the absence and presence of X, respectively. When appropriate

(16) The lifetime of the T_1 state of uranine was 33.8 μs, and its lifetime decreased to 1.0 μs with the quenching by TEA and to 1.6 μs with that by I^-. A detailed study is in progress.

(17) (a) Cowan, D. D.; Drisko, R. L. *J. Am. Chem. Soc.* **1967**, *89*, 3068. (b) Ferree, W. I., Jr.; Plummer, B. F.; Schloman, W. W., Jr. *J. Am. Chem. Soc.* **1974**, *96*, 7741. (c) $F(X)_{max}$ is defined as a saturated value of $F(X)$. $F(I^-)_{max}$ was easily obtained from Figure 6. $F(Br^-)$ and $F(Cl^-)$ under saturated concentration of Br^- and Cl^- were adopted as $F(Br^-)_{max}$ and $F(Cl^-)_{max}$, respectively.

(18) The spin–orbit coupling constants ($\zeta(X)$, kcal·mol^{-1} of unit) of the additives, X, were cited in: Turro, N. "Modern Molecular Photochemistry"; Benjamin: New York, 1978; p 118.

(19) (a) Horrocks, A. R.; Medinger, T.; Wilkinson, F. *Photochem. Photobiol.* **1967**, *6*, 21. (b) Horrocks, A. R.; Kearvell, A.; Tickle, K.; Wilkinson, F. *Trans. Faraday Soc.* **1966**, *62*, 3393. (c) Wilkinson et al. introduced the following equation:

$$(I_0/I) - 1 = [(\Phi_{TM}/\Phi°_{TM})(I_0/I) - 1]\Phi°_{TM} \quad (I)$$

where I_0, I, $\Phi°_{TM}$, and Φ_{TM} are fluorescence intensities and quantum yields of the excited triplet state in the absence and presence of heavy-atom additives, respectively. We tried to apply the analysis to the present hydrogen production enhanced by the external heavy-atom effect. Since the T_1 state is a precursor of the reduced dye with TEA, the hydrogen production rate is expected to be proportional to real Φ_{TM}. Therefore,

$$F(X) \propto \Phi_{TM}/\Phi°_{TM} \quad (II)$$

Combining eq I and II, we can obtain

$$(I_0/I) - 1 = [F(X)\cdot(I_0/I) - 1]\cdot\Phi°_{TM} \quad (III)$$

Scheme II. The Energetics of the Hydrogen Production with the Present Dye-Sensitized Particulate Sc/Pt Catalysts[a]

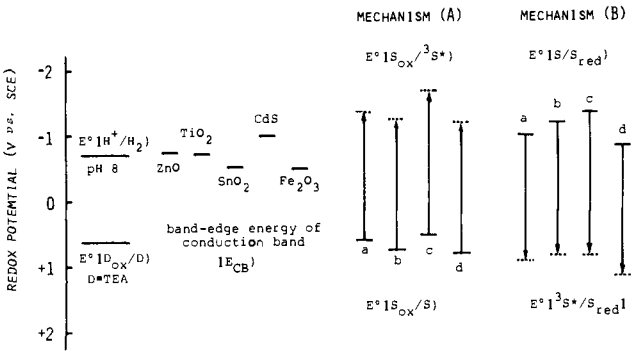

[a] A solid line and a dotted line show the relative positions of redox potentials in the ground state and the excited triplet one, respectively. The intervals of both potentials correspond to the excited triplet energy of the dyes (E_T): (a) rose bengal, (b) eosine bluish, (c) uranine, (d) rhodamine B.

concentrations of uranine and rhodamine B are used, both (I_0/I) and $F(X)$ were obtained for various concentrations of I^- and Br^-. There are good linear relationships between [(I_0/I) - 1] and [$F(X)(I_0/I)$ - 1], independent of I^- and Br^-, as is shown in Figure 7. The Φ°_{TM} evaluated from the slope was 0.14 for uranine and 0.0022 for rhodamine B, respectively. The success of the analysis demonstrated that T_1 states of the adopted dyes are precursors of the electron-injecting species, i.e., the reduced dye, which is confirmed by the transient absorption experiment (Figures 8 and 9).

A new absorption band at 393 nm was observed on illuminating the deaerated aqueous solution containing uranine (1.67×10^{-4} mol·L^{-1}) and TEA (3.3×10^{-1} mol·L^{-1}) without Sc/Pt (Figure 8). This 393-nm absorption band was assigned to a one-electron reduced uranine, uranine anion radical; see the work of Imamura.[20] The long lifetime (42 s) at pH 8 (Figure 9) and negative redox potential (E° (uranine/uranine anion radical) = −1.36 V vs. SCE) high enough to reduce a proton imply that the uranine anion radical is the electron-injecting species to Sc/Pt in this hydrogen production. Additional study of the photoreduction of uranine with I^-, TEA, or TEA-I^- systems was performed by using the transient absorption experiment. The initial absorbance changes at 393 nm after just 55 ms of illumination (488 nm) were 0.35, 0.04, and <0.01 for uranine–TEA–I^-, uranine–TEA, and uranine–I^- systems, respectively (Figure 9). The lifetime of uranine anion radical in all three cases had almost the same value (42 s) as obtained from the decays of absorbance at 393 nm followed by the first-order reaction.[21] These observations strongly suggested that uranine anion radical as an electron-injecting species into Sc/Pt is produced by the photoreduction of uranine with an electron donor and that the relative quantum yield of uranine anion radical generation is determined by the in situ Φ_{TM} of uranine and the reducing power of the adopted electron donor. As for the former, the addition of I^- enhanced the photoreduction of uranine up to 9 times, in agreement with the $F(I^-)_{max}$ of uranine shown in Figure 4. With respect to the latter, an irreversible electron donor such as TEA works as an efficient reductant for uranine, while a reversible electron donor such as I^- fails to reduce uranine. Since the standard redox potentials of TEA[22] and I^- are 0.64 and 0.27 V vs. SCE, the reducing power of a reductant is governed by its irreversibility rather than by its redox potential. That is to say, the back-electron transfer between the products, e.g., uranine anion radical and a one-electron oxidized donor, reduced the efficiency of the photoreduction.

(3) Energetics and Mechanism for Hydrogen Production. Scheme II shows the oxidative electron-transfer mechanism (A) and alternatively the reductive one (B), together with the redox potentials of the electron-injecting species of the adopted xanthene dyes and band-edge energy of the adopted Sc's. Both mechanisms involve the T_1 intermediate since the catalytic activity depends on the in situ Φ_{TM} of a xanthene dye and is enhanced by the heavy-atom effect

$$S \xrightarrow{h\nu} {}^1S^* \quad (4)$$

$${}^1S^* \rightarrow {}^3S^* \quad (5)$$

$$\text{(A)} \begin{cases} {}^3S^* + 1I^+ \xrightarrow{Sc/Pt} S_{ox} + {}^1/_2H_2 & (6) \\ S_{ox} + D \rightarrow S + D_{ox} & (7) \end{cases}$$

$$\text{(B)} \begin{cases} {}^3S^* + D \rightarrow S_{red} + D_{ox} & (8) \\ S_{red} + H^+ \xrightarrow{Sc/Pt} S + {}^1/_2H_2 & (9) \end{cases}$$

where the abbreviations are shown in the caption of Scheme II. Both mechanisms, A and B, succeed in including (i) the electron injection process to Sc/Pt and (ii) the regeneration process of S_{ox} or S_{red} to S. The electron-injecting species, $^3S^*$ for mechanism A and S_{red} for mechanism B, must have redox potentials large enough to reduce the protons to hydrogen at pH 8 (eq 10 and 12). Also in the regeneration process, the oxidant, S_{ox} for mechanism A and $^3S^*$ for mechanism B, must oxidize a sacrificial electron donor (TEA) (eq 11 and 13). These conditions require

$$\text{(A)} \begin{cases} E^\circ(S_{ox}/{}^3S^*) < E^\circ(H^+/H_2) = -0.71 \text{ V} & (10) \\ E^\circ(S_{ox}/S) > E^\circ(D_{ox}/D) = 0.64 \text{ V} & (11) \end{cases}$$

$$\text{(B)} \begin{cases} E^\circ(S/S_{red}) < E^\circ(H^+/H_2) = -0.71 \text{ V} & (12) \\ E^\circ({}^3S^*/S_{red}) > E^\circ(D_{ox}/D) = 0.64 \text{ V} & (13) \end{cases}$$

where E° (oxidant/reductant) is the standard redox potential toward SCE. $E^\circ(S_{ox}/S)$, $E^\circ(S/S_{red})$, and $E^\circ(D_{ox}/D)$ are obtained by using cyclic voltammetry, and $E^\circ(S_{ox}/{}^3S^*)$ and $E^\circ({}^3S^*/S_{red})$ are estimated by using eq 14 and 15

$$E^\circ(S_{ox}/{}^3S^*) = E^\circ(S_{ox}/S) - E_T \quad (14)$$

$$E^\circ({}^3S^*/S_{red}) = E^\circ(S/S_{red}) + E_T \quad (15)$$

where E_T is the excited triplet-state energy of a xanthene dye. The energetics favor the reductive electron-transfer mechanism B rather than the oxidative one A. This conclusion is based on the idea that all xanthene dyes having some catalytic activities satisfy (12) and (13) but not (10) and (11). So, for example, with uranine, the confirmation of the presence of uranine anion radical with a much longer lifetime (42 s) than that of $^3S^*$ (10^{-6}–10^{-5} s)[23] suggests that S_{red} plays a role in injecting an electron to the particulate Sc/Pt and that $^3S^*$ is a precursor of S_{red}. The difference in the lifetimes of the electron-injecting species in both mechanisms A and B leads to the following significant consideration: The amount of dye effectively participating in the reductive electron transfer is much larger than that in the oxidative one. Therefore, the apparent quantum yield of hydrogen production via mechanism B exceeds by far than via mechanism A. Actually, in a dye-sensitized semiconductor *bulky* electrode (rose bengal–ZnO sinter electrode),[7,24] an apparent current quantum efficiency of 1% has been reported, which is governed by the oxidative electron-transfer mechanism. The intrinsic current quantum efficiency was evaluated to be 22%, assuming that only rose bengal adsorbed on the ZnO sinter electrode contributes to the effective photocurrent. The high quantum yield of hydrogen production in the present work is explained by mechanism B where most of the dye in the photolysis solution can take part in the reductive electron transfer because of the long lifetime of S_{red}.

The present study proposes mechanism B with its energetics in the homogeneous region mainly focussing on the photoreactions

(20) (a) Imamura, M.; Koizumi, M. *Bull. Chem. Soc. Jpn.* **1955**, *28*, 117; **1956**, *29*, 899, 913. (b) Imamura, M. *Bull. Chem. Soc. Jpn.* **1956**, *31*, 62, 962.

(21) A detailed study on the time dependence of the transient absorption spectrum of uranine anion radical, especially with an extended time region (~60 sec), has shown that the decay of the absorbance at 393 nm obeyed first-order kinetics.

(22) The potential at which an anodic current was built up was adopted as a redox potential of TEA.

(23) Sugita, K. Graduate Thesis, Mie University, 1984.

(24) The dynamic process of dye sensitization with use of a *bulky* semiconductor electrode has been recently clarified. Kojima, T.; Ban, T.; Kasatani, K.; Kawasaki, M.; Sato, H. *Chem. Phys. Lett.* **1982**, *91*, 319.

Table III. Summary of Hydrogen Production with Xanthene Dye Sensitized Semiconductor Powder Catalyst Driven by Visible-Light Illumination[a]

sensitizer	additive	Φ_{TM}	Φ_{H_2}	$\Phi_{dehalogenation}$	heavy-atom effect
nonhalogenated xanthene dye	none	small	small	little	none
heavy-halogenated xanthene dye	none	large	large	large	internal
nonhalogenated xanthene dye	heavy atom	large	large	little	external

[a] Φ_{TM}, Φ_{H_2}, and $\Phi_{dehalogenation}$ are the in situ excited triplet quantum yield of a xanthene dye, the apparent quantum yield of hydrogen production with a xanthene dye sensitized Sc/Pt catalyst, and the quantum yield of dehalogenation of a xanthene dye.

of the dye. However, there still remains the proton-reducing process with the particulate Sc/Pt. The significant question is whether the semiconductor in particulate Sc/Pt catalyst plays a role in an electron relay or whether the band structure of Sc is essential for the catalytic actions of the Sc/Pt. This question is involved in the proton-reducing process after the electron injection to the Sc/Pt. If Sc acts as an electron relay (see route I, below), the band structure must satisfy the energetics requirement (eq 18).

$$\text{route I} \begin{cases} S_{red} + \text{Sc/Pt} \rightarrow S + e^- \text{ in Sc/Pt} & (16) \\ e^- \text{ in Sc/Pt} + H^+ \xrightarrow{\text{Pt}} {}^1/_2H_2 & (17) \\ E_{CB} < E^\circ(H^+/H_2) = -0.71 \text{ V} & (18) \end{cases}$$

$$\text{route II} \quad S_{red} + H^+ \xrightarrow[\text{independent of Sc}]{\text{Pt}} S + {}^1/_2H_2 \quad (19)$$

Otherwise, if not, eq 18 is irrelevant. Adopting Pt colloid, SiO_2/Pt, and Al_2O_3/Pt in lieu of Sc/Pt, a slight amount of hydrogen was produced (<0.03 μmol·min^{-1}), similar to the so-called two-component catalyst system without any electron relays.[25]

Two types of time dependence of hydrogen production in the dark were shown, preliminarily, when a reducing agent, such as $Na_2S_2O_4$ (E° = −1.38 V) or methylviologen cation radical (E° = −0.69 V), was added to the deaerated aqueous solution (pH 6) containing suspended Sc/Pt with stirring. The Sc/Pt satisfying eq 18 such as ZnO/Pt, TiO_2/Pt, and CdS/Pt resulted in gradual hydrogen production for over 10 h with up to 20–60% of conversion, while the Fe_2O_3/Pt, SnO_2/Pt, Pt colloid, and SiO_2/Pt resulted in slight hydrogen production (1–5% of conversion within 20 min). The distinct difference between these time courses must result from the existence of a band structure for the semiconductor satisfying the conditions of route I. A posteriori consideration shows that an immediate proton reduction to hydrogen would originate from route II directly induced by the catalytic action of the dispersed Pt and that, alternatively, a gradual hydrogen production would proceed by route I. The latter (route I) had a higher yield of hydrogen production than the former (route II), which is presumed to result from the electron-accumulating function of the supporting Sc in its specific conduction band. However, the high catalytic activity of Fe_2O_3 (Table I), whose band structure does not satisfy the requirement in (18), drew much attention. This should be considered on the basis not only of the degree of Pt dispersion on the support but also of the so-called quasi-Fermi level[26] which is governed by the in situ electron-injected particulate Sc/Pt. Recently, it has been pointed out independently by A. J. Bard and M. Grätzel that a particulate Sc photocatalyst with its band-gap excitation has an extraordinariness in its photoredox actions, and is different from those of a Sc *bulky* electrode.[27] When only the positive holes of the photogenerated electron-hole pair are immediately scavenged by a reducing agent, the remaining electrons in the conduction band shift, temporarily, the band energy in a negative direction. This is classified as a quasi-Fermi level. Also in the present dye sensitization, the excess electrons injected from the dyes bring about a similar phenomena, so that even Fe_2O_3/Pt acts as a proton-reducing catalyst following route I. A detailed study of the proton-reducing process with particulate Sc/Pt is in progress.

Scheme III. The Mechanism of the Visible-Light-Induced Water Reduction with the Present Dye-Sensitized Particulate Sc/Pt Catalyst[a]

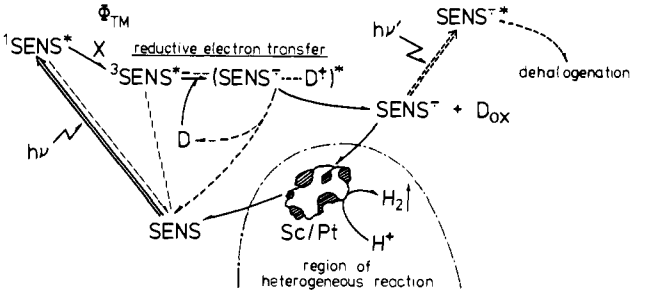

[a] SENS, D, and X are a dye, an electron donor, and a heavy-atom additive, respectively. Solid lines and broken lines show desired hydrogen-production processes and undesired other processes such as a thermal back-electron transfer process, deactivation one, and a photodehalogenation one.

In conclusion, the reductive electron-transfer mechanism B through the T_1 state of the dye is proposed (Scheme III). The present hydrogen production is classified in Table III. Heavy-halogenated xanthene dyes, e.g., rose bengal, erythrosine, and eosine bluish, have high quantum yields of hydrogen production but tend to photodehalogenate, while nonhalogenated xanthene dyes, e.g., uranine and rhodamine B, have high durability against any photodeterioration but have moderate catalytic activites. The present improved catalyst, i.e., uranine or rhodamine B–Sc/Pt–I^-–TEA, has the pronounced advantages of high quantum yield and high durability, which are acquired through the use of durable dyes and the application of the external heavy-atom effect. This approach to the design of a dye-sensitized water-reduction catlayst is both theoretically sound and practically effective.

Acknowledgment. We are grateful to Prof. Hiroyasu Sato, Prof. Masahiro Kawasaki, Dr. Kazuo Kasatani, and Kazuki Sugita, Mie University, for their measurements of the transient absorption spectra and valuable discussion. We also thank Dr. Kazuhito Hashimoto, Institute of Molecular Science, for valuable suggestion. This work was partially supported by Grand-in-Aid for Scientific Research from the Ministry of Education of Japan.

Registry No. ZnO, 1314-13-2; TiO_2, 13463-67-7; SnO_2, 18282-10-5; CdS, 1306-23-6; Fe_2O_3, 1309-37-1; Pt, 7440-06-4; H_2, 1333-74-0; H_2O, 7732-18-5; TEA, 102-71-6; rose bengal, 632-69-9; eosine bluish, 548-24-3; uranine, 518-47-8; rhodamine B, 81-88-9; erythrosine, 16423-68-0.

(25) Harrimann, A.; Richoux, M.-C. *J. Photochem.* **1981**, *15*, 335.
(26) Gerischer, H. *J. Electrochem. Soc.* **1966**, *113*, 1174; **1977**, *133*, 82.
(27) (a) Ward, M. D.; White, J. R.; Bard, A. J. *J. Am. Chem. Soc.* **1983**, *105*, 27. (b) Duonhong, D.; Ramsden, J.; Grätzel, M. *J. Am. Chem. Soc.* **1982**, *104*, 2977.